Structure and Stability of Alkane−Linked DNA Hairpin Conjugates

ARTICLE *in* THE JOURNAL OF ORGANIC CHEMISTRY · SEPTEMBER 2010

Impact Factor: 4.72 · DOI: 10.1021/jo1013299 · Source: PubMed

3 AUTHORS:

Mahesh Hariharan
Indian Institute Of Science Education and Re…
45 PUBLICATIONS **843** CITATIONS
SEE PROFILE

Karsten Siegmund
Northwestern University
16 PUBLICATIONS **192** CITATIONS
SEE PROFILE

Frederick D Lewis
Northwestern University
319 PUBLICATIONS **9,213** CITATIONS
SEE PROFILE

JOC Article
pubs.acs.org/joc

Structure and Stability of Alkane-Linked DNA Hairpin Conjugates

Mahesh Hariharan,*[,‡] Karsten Siegmund,[†] and Frederick D. Lewis*[,†]

[†]*Department of Chemistry, Northwestern University, Evanston, Illinois 60208-3113, and* [‡]*School of Chemistry, Indian Institute of Science Education and Research, Thiruvananthapuram, Kerala, India 695 016*

mahesh@iisertvm.ac.in; fdl@northwestern.edu

Received July 6, 2010

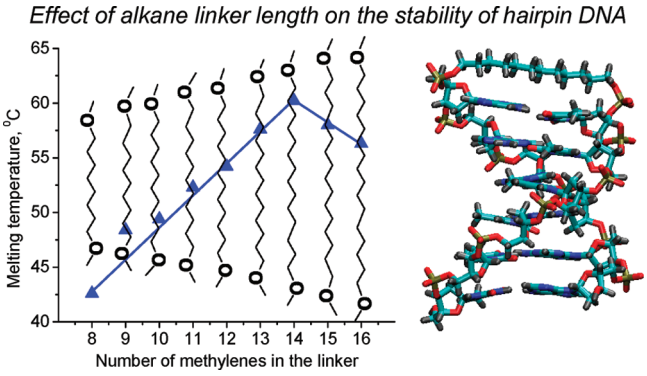

The synthesis and properties of three related families of alkane-linked DNA hairpins are reported. The first possesses a dodecane linker (C12) and 2−8 AT base pairs. The second possesses six AT base pairs and straight chain alkane linkers having 8−16 methylenes. The third has three alkane linkers of different length and a constant six base-pair stem with alternating A-T bases and a single TT step. The spectroscopic properties (UV, CD, and ^{1}H NMR) and molecular modeling are consistent with the formation of base-paired B-DNA structures for all hairpins having four or more AT base pairs. The thermal stability of hairpins having a C12 linker is greater than that of the commonly used hexa(ethylene glycol) linker but less than that of the stilbenediether linker having the same AT base-pair domain. Hairpin stability is related to both hydrophobic interactions between the linker and the adjacent base pair (stilbene > alkane > glycol) and the overall length of the linker. The stability of the alkane-linked hairpins having six AT base pairs is greater for a tetradecane linker than for either shorter or longer linkers. The good thermal stability of alkane-linked hairpins and absence of a chromophore which absorbs in the UV region makes them well-suited for studies of the electronic spectra and photochemistry of short hairpins having variable base-pair sequences.

Introduction

Single-stranded DNA and RNA can form hairpin structures in which a base-paired duplex stem is connected by a loop region possessing unpaired bases.[1,2] Hairpin structures play an important role in biological processes and also provide simple model systems for the investigation of base pairing in short duplex domains. The thermodynamic stability of natural hairpins is determined by both the stem and loop regions.[3] The formation of stable mini-hairpins possessing two G-C base pairs connected by a trinucleotide loop has been reported for d(GCGAAGC) and several related sequences.[4] Loop replacement by non-natural

(1) Bloomfield, V. A.; Crothers, D. M.; Tinoco, I. *Nucleic Acids. Structures, Properties, and Functions*; University Science Books: Sausalito, CA, 2000.

(2) Neidle, S. *Oxford Handbook of Nucleic Acid Structure*; Oxford University Press: Oxford, 1999.

(3) (a) Senior, M. M.; Jones, R. A.; Breslauer, K. J. *Proc. Natl. Acad. Sci. U.S.A.* **1988**, *85*, 6242–6246. (b) Hardin, J. W.; Batey, R. T. *Structure* **2004**, *12*, 731–732. (c) Blommers, M. J. J.; Walters, J.; Haasnoot, C. A. G.; Aelen, J. M. A.; Vandermarel, G. A.; Vanboom, J. H.; Hilbers, C. W. *Biochemistry* **1989**, *28*, 7491–7498. (d) Shen, Y. Q.; Kuznetsov, S. V.; Ansari, A. *J. Phys. Chem. B* **2001**, *105*, 12202–12211. (e) Kuznetsov, S. V.; Shen, Y. Q.; Benight, A. S.; Ansari, A. *Biophys. J.* **2001**, *81*, 2864–2875.

(4) (a) Hirao, I.; Kawai, G.; Yoshizawa, S.; Nishimura, Y.; Ishido, Y.; Watanabe, K.; Miura, K. *Nucleic Acids Res.* **1994**, *22*, 576–582. (b) Yoshizawa, S.; Kawai, G.; Watanabe, K.; Miura, K.; Hirao, I. *Biochemistry* **1997**, *36*, 4761–4767.

Published on Web 08/26/2010 DOI: 10.1021/jo1013299

CHART 1. Structures of the Linkers Sd2 and EG6 Used in Previous Studies of Synthetic DNA Hairpins

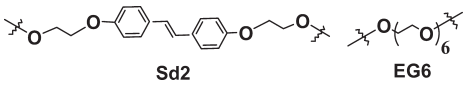

linkers has been employed for the synthesis of stable mini-hairpins.[5,6] For example, base-paired structures have been reported for mini-hairpins possessing stilbenediether linkers (Sd2, Chart 1) connecting two or more A-T or G-C base pairs.[7−10]

Our interest in the electronic spectra[11] and photochemistry[12,13] of short DNA duplexes led us to investigate the stability of nonchromophoric hairpin linkers that would not compete with natural bases for the absorption of ultraviolet irradiation. The most widely studied of such linkers is hexa(ethylene glycol) EG6 (Chart 1).[14,15] Rumney and Kool investigated the thermodynamic stability of a series of hairpins possessing a conserved 6-base-pair stem and loops consisting of 3−8 ethylene glycol units and found that the hepta(ethylene glycol) linker formed the most stable hairpin.[16] Similar results were reported by Pils and Micura for RNA hairpins possessing a 4-base-pair stem.[17] Oligo(ethylene glycol) linkers were also employed in our studies on the stability and structural dynamics of DNA hairpin and dumbbell conjugates possessing poly(dA)-poly(dT) base-pair domains consisting of 4−10 base pairs.[18]

The synthesis and properties of a DNA dumbbell possessing a 16-base-pair duplex connected by two C12 alkane (dodecyl) linkers was reported by Doktycz et al.[19] The enhanced thermodynamic stability of this dumbbell compared to an analogue possessing T_4 linkers was attributed to hydrophobic interactions between the linker and adjacent

CHART 2. Structures of Oligomethylene-Linked DNA Hairpin Conjugates and Enlargement of the C12 Linker Region[a]

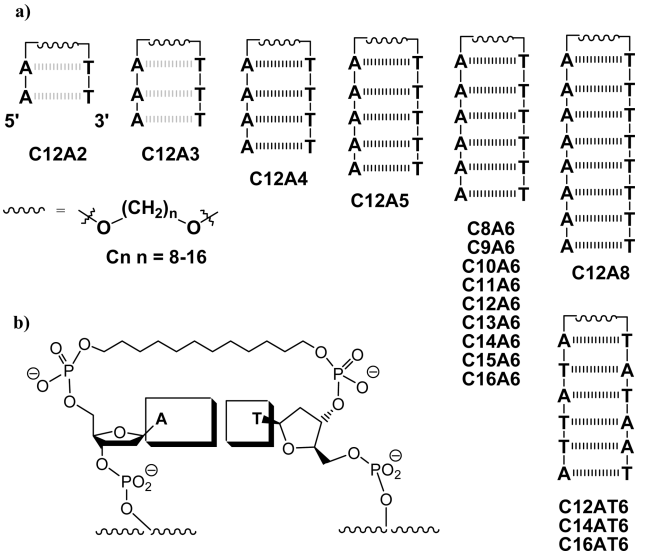

[a](a) Oligomethylene-linked DNA hairpin conjugates having C*n* alkane linkers (n = 6−16) and either poly(dA)-poly(dT) stems (A*m*, m = 2−6 or 8) or a mixed base sequence stem (AT6). Weak hydrogen bonds are shown with grey dashes, stronger hydrogen bonds with dark dashes. (b) Enlargement of the C12 linker region showing a C12 linker connecting an A−T base pair.

base pairs.[20] The predominantly *anti* alkane conformation suggested for the linker would provide a better match for the normal B-DNA dimensions than would a conformation possessing multiple gauche-butane conformations. In addition to hydrophobic association, the alkane linker offers the ability to vary the length of the linker incrementally by a single carbon atom, as opposed to the 3-atom increments of oligo(ethylene glycol). We have used the C12 linker in our studies of the electronic spectra[11] and T-T photodimerization in short base-pair domains.[12]

We report here an investigation of the synthesis and properties of three related series of alkane-linked DNA hairpins (Chart 2). The first series consists of hairpins possessing the C12 linker and a poly(dA)-poly(dT) stem consisting of 2−8 A-T base pairs. This series allows for comparison of hairpin stabilities with those of hairpins having EG6 and Sd2 linkers.[9,18] Poly(dT) sequences are also of interest as "hot-spots" for TT photodimerization.[21] The greater stability of mini-hairpins having alkane versus EG6 linkers makes them better suited for studies of very short base-pair domains. The second series has a constant $(dA)_6$-$(dT)_6$ base-pair stem and C*n* linkers possessing 6−16 methylenes. This series permits determination of the optimum length for an alkane linker. We find that the alkane linker has little effect on the electronic spectra of the base-pair domains but has a significant effect on the stability of the hairpins. The third series has three different C*n* linkers and a constant 6-base-pair stem with alternating A-T bases and a single TT step. The C12-linked member of this series is reported to undergo photodimerization at its TT step.[12]

(5) (a) Salunkhe, M.; Wu, T.; Letsinger, R. L. *J. Am. Chem. Soc.* **1992**, *114*, 8768–8772. (b) Benseler, F.; Fu, D.-J.; Ludwig, J.; McLaughlin, L. W. *J. Am. Chem. Soc.* **1993**, *115*, 8483–8484. (c) Durand, M.; Chevrie, K.; Chassignol, M.; Thuong, N. T.; Maurizot, J. C. *Nucleic Acids Res.* **1990**, *18*, 6353–6359. (d) Thomson, J. B.; Tuschl, T.; Eckstein, F. *Nucleic Acids Res.* **1993**, *21*, 5600–5603. (e) Williams, D. J.; Hall, K. B. *Biochemistry* **1996**, *35*, 14665–14670. (f) Benseler, F.; Fu, D. J.; Ludwig, J.; McLaughlin, L. W. *J. Am. Chem. Soc.* **1993**, *115*, 8483–8484. (g) Hariharan, M.; Zheng, Y.; Long, H.; Zeidan, T. A.; Schatz, G. C.; Vura-Weis, J.; Wasielewski, M. R.; Zuo, X. B.; Tiede, D. M.; Lewis, F. D. *J. Am. Chem. Soc.* **2009**, *131*, 5920–5929.

(6) Letsinger, R. L.; Wu, T. *J. Am. Chem. Soc.* **1995**, *117*, 7323–7328.

(7) Lewis, F. D.; Liu, X. *J. Am. Chem. Soc.* **1999**, *121*, 11928–11929.

(8) Lewis, F. D.; Liu, X.; Wu, Y.; Miller, S. E.; Wasielewski, M. R.; Letsinger, R. L.; Sanishvili, R.; Joachimiak, A.; Tereshko, V.; Egli, M. *J. Am. Chem. Soc.* **1999**, *121*, 9905–9906.

(9) Lewis, F. D.; Wu, Y.; Liu, X. *J. Am. Chem. Soc.* **2002**, *124*, 12165–12173.

(10) Egli, M.; Tereshko, V.; Mushudov, R.; Sanishvili, R.; Liu, X.; Lewis, F. D. *J. Am. Chem. Soc.* **2003**, *125*, 10842–10849.

(11) Burin, A. L.; Armbruster, M. E.; Hariharan, M.; Lewis, F. D. *Proc. Natl. Acad. Sci. U.S.A.* **2009**, *106*, 989–994.

(12) Hariharan, M.; Lewis, F. D. *J. Am. Chem. Soc.* **2008**, *130*, 11870–11871.

(13) McCullagh, M.; Hariharan, M.; Lewis, F. D.; Markovitsi, D.; Douki, T.; Schatz, G. C. *J. Phys. Chem. B* **2010**, *114*, 5215–5221.

(14) Altmann, S.; Labhardt, A. M.; Bur, D.; Lehmann, C.; Bannwarth, W.; Billeter, M.; Wuthrich, K.; Leupin, W. *Nucleic Acids Res.* **1995**, *23*, 4827–4835.

(15) (a) Tarkoy, M.; Phipps, A. K.; Schultze, P.; Feigon, J. *Biochemistry* **1998**, *37*, 5810–5819. (b) Jiang, L. H.; Russu, I. M. *Nucleic Acids Res.* **2001**, *29*, 4231–4237.

(16) Rumney, S.; Kool, E. T. *J. Am. Chem. Soc.* **1995**, *117*, 5635–5646.

(17) (a) Pils, W.; Micura, R. *Nucleic Acids Res.* **2000**, *28*, 1859–1863. (b) Ebert, M. O.; Jaun, B.; Pils, W.; Micura, R. *Helv. Chim. Acta* **2000**, *83*, 2336–2343.

(18) McCullagh, M.; Zhang, L.; Karaba, A. H.; Zhu, H.; Schatz, G. C.; Lewis, F. D. *J. Phys. Chem. B* **2008**, *112*, 11415–11421.

(19) Doktycz, M. J.; Paner, T. M.; Benight, A. S. *Biopolymers* **1993**, *33*, 1765–1777.

(20) Doktycz, M. J.; Goldstein, R. F.; Paner, T. M.; Gallo, F. J.; Benight, A. S. *Biopolymers* **1992**, *32*, 849–864.

(21) (a) Bourre, F.; Renault, G.; Seawell, P. C.; Sarasin, A. *Biochimie* **1985**, *67*, 293–299. (b) Becker, M. M.; Wang, Z. *J. Mol. Biol.* **1989**, *210*, 429–438.

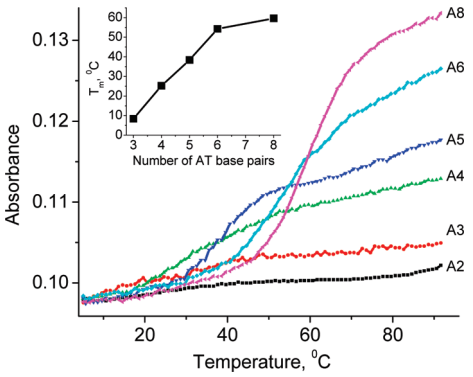

FIGURE 1. Thermal dissociation profiles for C12-linked hairpin conjugates having different number of AT base pairs in 10 mM phosphate buffer (pH 7.2) containing 100 mM NaCl. Concentrations of the hairpin conjugates used: **C12A2** (2.3 μM); **C12A3** (1.6 μM); **C12A4** (1.2 μM); **C12A5** (0.9 μM); **C12A6** (0.81 μM); and **C12A8** (0.6 μM).

TABLE 1. Melting Points for Conjugates C12A*n* (see Chart 2 for structures) and for EG6- and Sd2-linked DNA Hairpin Conjugates Containing a Variable Number of AT Base Pairs (n = 2, 3, 4, 5, 6, and 8)

	T_m, °C		
n[a]	C12[b]	EG6[c]	Sd2[d]
2			30.0
3	8.4		46.7
4	25.2	29.0	54.0
5	39.3	40.0	
6	54.2	44.0	64.2
8	59.7	52.0	

[a]Number of AT base pairs. [b]T_m values determined from the derivative of the 260 nm UV thermal dissociation profiles. [c]Data from ref 18. [d]Data from ref 9.

Results

Electronic Spectra and Thermal Stability of Alkane-Linked Hairpin Conjugates. Methods employed for the synthesis and characterization of the alkane-linked hairpin conjugates from the α,ω-alkanediols are described in the Experimental Section.[9,12] The UV and CD spectra of conjugates **C12A4**, **C12A6**, and **C12A8** have previously been reported.[11] All of the conjugates display a broad ultraviolet absorption band at 260 nm similar to that of the corresponding EG-linked hairpins.[9] The spectra of several representative alkane-linked conjugates are shown in Figure S1, Supporting Information.

Thermal dissociation profiles for the C12-linked hairpin conjugates having a variable number of AT base pairs (C12An, Chart 2) are shown in Figure 1. The C12-linked hairpin sequences containing 4, 5, 6, and 8 AT base pairs show sigmoidal behavior with increasing transition temperature as the stem length increases (Table 1); however, the hairpin conjugates containing 2 and 3 AT base pairs do not display resolved melting transitions. Melting temperatures (T_m) obtained from the first derivatives of these profiles are reported in Table 1 and shown in the inset to Figure 1. Also reported in Table 1 are published data for hairpins having EG6[18] and Sd2 linkers.[9] All of these conjugates adopt hairpin rather than duplex structures at the low concentrations employed in these studies.

Thermal dissociation profiles monitored at 260 nm for **C8A6**−**C16A6** in 10 mM phosphate buffer (pH 7.2) containing 100 mM NaCl are shown in Figure 2. The melting curves for even-numbered alkane linkers display continuous hyperchromicity even at temperatures above the melting transition (Figure 2a), whereas the melting curve for odd-numbered alkane-linker-containing hairpin sequences show no increase in hyperchromicity at temperatures above the melting transitions (Figure 2b). Values of T_m obtained from the derivative of the thermal dissociation profiles (Figure 2a and b, insets) are reported in Table 2. A plot of T_m versus the number of carbon atoms in the alkane linker shown in Figure 3 shows a maximum value for the C14 linker.

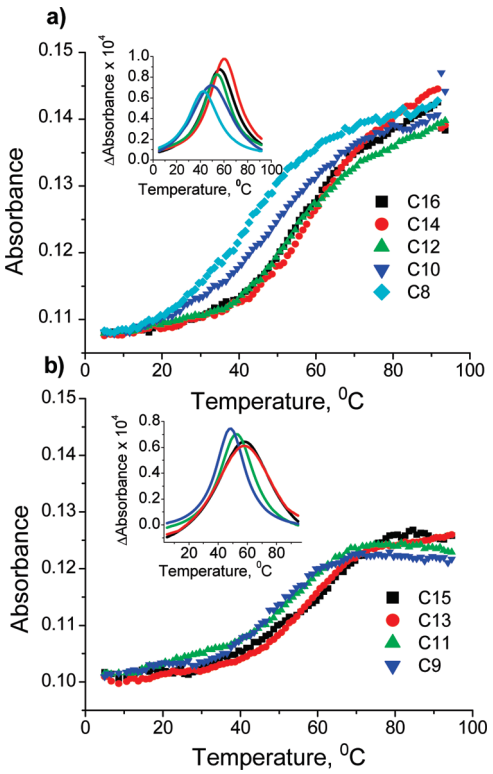

FIGURE 2. Thermal dissociation profiles for the alkane-linked hairpins **C8A6**−**C16A6** (see Chart 2 for structures) having an even (a) or odd (b) number of carbons in 10 mM phosphate buffer (pH 7.2) containing 100 mM NaCl. Insets show first derivatives of thermal dissociation profiles.

TABLE 2. Melting Temperatures Obtained from UV and CD Spectra and Calculated P−P Distances for the Conjugates C8A6−C16A6 (See Chart 2 for Structures)

linker	T_m,[a] °C	T_m,[b] °C	P−P distance, Å[c]
C8	42.6		14.2
C9	48.4	47.4	15.5
C10	49.4		16.8
C11	52.3	52.3	18.0
C12	54.2	54.6	19.3
C13	57.6		20.6
C14	60.2	59.9	21.9
C15	58.0		23.1
C16	56.3		24.4
Sd2	64.2[d]		21.9
EG6	44.0[e]		23.8

[a]T_m values determined from the derivative of the 260 nm UV thermal dissociation profile. [b]T_m values determined using ellipticity at 280 nm. [c]Calculated distance between phosphorus atoms attached to the linker in its fully extended, all-*anti* conformation (see text). [d]Data from ref 9. [e]Data from ref 18.

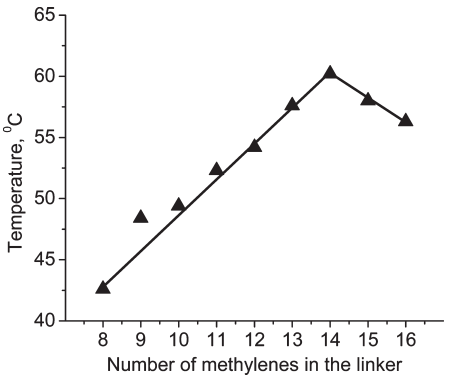

FIGURE 3. DNA melting temperature (T_m) versus the number of methylenes in the linker for conjugates **C*n*A6** (see Chart 2 for structures).

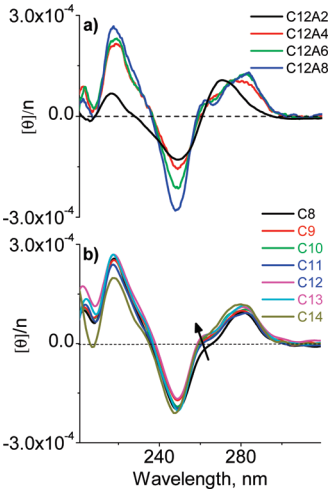

FIGURE 4. Circular dichroism spectra of (a) **C12A*m*** conjugates having different numbers of AT base pairs (m = 2, 4, 6, and 8 layers) and (b) **C*n*A6** conjugates having different alkane linkers (n = 8−14) in 10 mM phosphate buffer (pH 7.2) containing 100 mM NaCl. Arrow indicates the increase in ellipticity at 260 nm with increasing length of the linker.

The lengths of fully extended (all-*anti*) alkane linkers were determined by constructing the alkane PO_4-(CH_2)-PO_4 linkers alone, without any attached nucleotides, in Macromodel[22] and optimizing the all-*anti* alkane structures using a MM2 force-field. The P−P distances obtained by this procedure are reported in Table 2. Each additional methylene group results in a 1.25 Å increase in the P−P distance.

Circular Dichroism Spectra. The circular dichroism (CD) spectra of conjugates **C12A2**, **C12A4**, **C12A6**, and **C12A8** are shown in Figure 4a. CD maxima near 220 and 280 nm and a minimum near 250 nm are observed for conjugates possessing 2 or more AT base pairs, and an additional maximum at 260 nm is observed for hairpins possessing six or more AT base pairs. Conjugate **C12A2** exhibits a broader CD spectrum with maxima at 225 and 268 nm and minimum at 247 nm. The CD spectra of conjugates **C8A6**−**C14A6** that possess six AT base pairs and different alkane linkers are shown in Figure 4b. All of these spectra exhibit maxima near 220 and 280 nm and a minimum near 250 nm. The strength of the 260 nm shoulder increases with the length of the alkane linker.

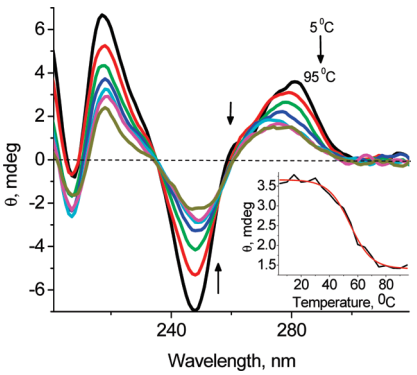

FIGURE 5. Temperature-dependent circular dichroism spectra of conjugate **C12A6** in 10 mM phosphate buffer (pH 7.2) containing 100 mM NaCl. Inset shows the decrease in ellipticity at 280 nm with increase in temperature. Arrows indicate the change in temperature from 0 to 95 °C.

The temperature-dependent circular dichroism spectra of conjugate **C12A6** is shown in Figure 5. The intensities of all bands decrease, and the 280 maximum shifts to shorter wavelengths, accompanied by loss of the 260 nm shoulder, upon heating. Similar behavior was observed for sequences containing different linker lengths (9−16 methylenes) (Figures S2−S4, Supporting Information). The derivative of a plot of the CD intensity at 280 nm versus temperature for **C12A6** provides a value of T_m = 54 °C (Figure 5, inset), in good agreement with the T_m value obtained from temperature-dependent UV absorption measurements. The CD melting temperatures for several of the hairpins are reported in Table 2.

1D ^{1}H NMR Spectroscopy. Proton NMR spectra for conjugates **C12A4**, **C12A6**, and **C12A8** at several temperatures between 5 and 40 °C in the spectral regions 13−15 ppm (imino protons) and 0−2 ppm (alkane linker and thymine methyl protons) are shown in Figures 6 and 7, respectively. Spectra for the 7−8.4 ppm spectral region (aromatic protons) is shown in Figure S8 (Supporting Information). The signals for hydrogen-bonded imino protons in water are expected in the chemical shift range from 13 to 15 ppm. In this chemical shift range (Figure 6), two weak signals are observed for **C12A4** at 5 °C, whereas for **C12A6** four out of six possible imino proton signals can be seen (two of them with the same chemical shift) and for **C12A8** at least six out of eight imino protons are visible. Increasing temperature results in broadening and loss of signal intensity. In the region from 0 to 2 ppm (Figure 7) as many as 10 signals can be distinguished for the 10 central methylenes (20 protons) of the C12 linker, in addition to the stronger singlets for the thymine methyls. Some of these signals have peak areas corresponding to a single hydrogen atom. The two methylenes attached to oxygen are expected in the region around 3.5 ppm, which also contains the signals of the deoxyribose 3′- and 4′-protons (data not shown). In the aromatic region from 7 to 9 ppm, most of the aromatic protons for **C12A4**, **C12A6**, and **C12A8** can be identified (Figure S8 in Supporting Information). Pronounced line-broadening[23] is observed for several of

(22) Mohamadi, F.; Richards, N. G. J.; Guida, W. C.; Liskamp, R.; Lipton, M.; Caufield, C.; Chang, G.; Hendrickson, T.; Still, W. C. *J. Comput. Chem.* **1990**, *11*, 440–467.

(23) He, G. Y.; Patra, A.; Siegmund, K.; Peter, M.; Heeg, K.; Dalpke, A.; Richert, C. *ChemMedChem* **2007**, *2*, 549–560.

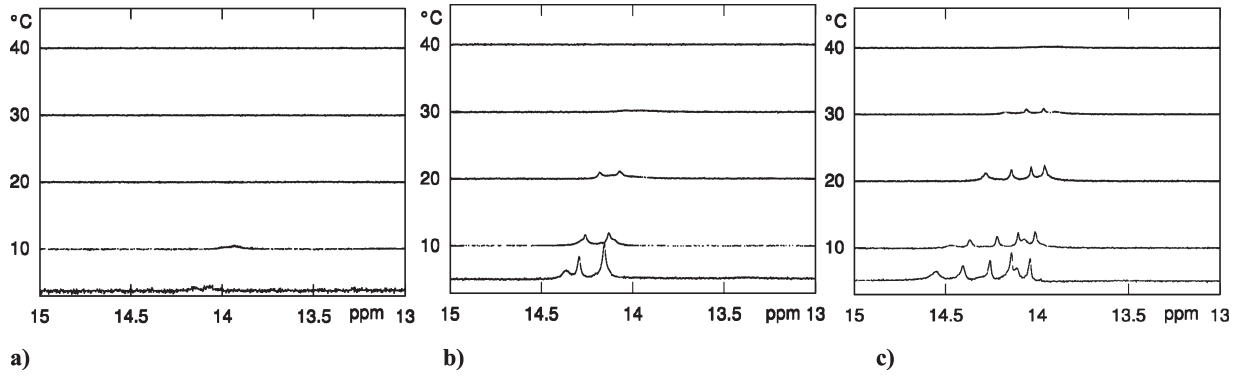

FIGURE 6. Temperature-dependent 1D NMR spectra for the thymine H3 imino protons of conjugates (a) **C12A4**, (b) **C12A6**, and (c) **C12A8** in 90% H_2O/10% D_2O with 10 mM phosphate buffer and 100 mM NaCl at temperatures between 5 and 40 °C .

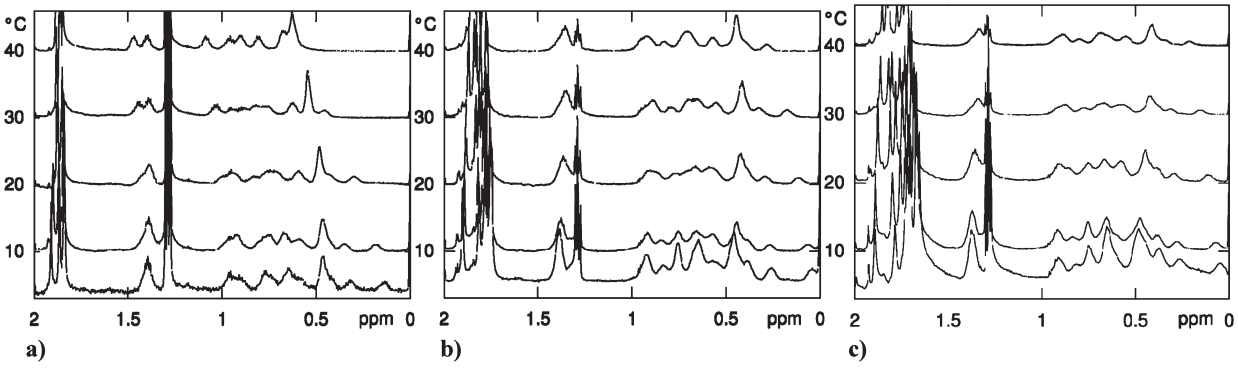

FIGURE 7. Temperature-dependent 1D NMR spectra for the C12 linker and thymine methyl protons of conjugates (a) **C12A4**, (b) **C12A6**, and (c) **C12A8** in 90% H_2O/10% D_2O with 10 mM phosphate buffer and 100 mM NaCl at temperatures between 5 and 40 °C.

the aromatic protons of **C12A4** at low temperature, whereas **C12A6** and **C12A8** show no such selective line-broadening. Assignment of the DNA and linker proton resonances would require 2D NMR experiments that were not attempted.

1D ^{1}H NMR measurements have also been carried out for hairpins **C12AT6**, **C14AT6**, and **C16AT6** linkers which have 5′-ATTATA base sequences rather than A-tracts (Chart 2). The temperature-dependent spectra for the imino proton region is shown in Figure 8. In the case of the C14 linker all six imino protons are observed at 5 °C and five of these are visible up to a temperature of 25 °C. In the case of the C12 and C14 linkers five of the six imino protons are observed at 5 °C, none of which can be resolved at 25 °C.

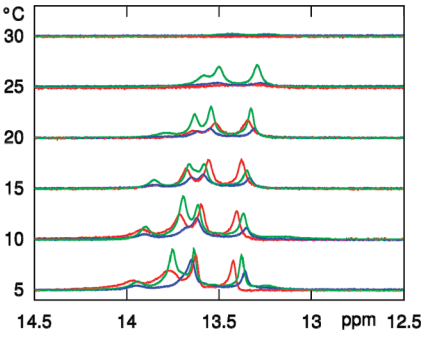

FIGURE 8. Temperature-dependent 1D NMR spectra for the thymine H3 imino protons of conjugates **C12AT6** (red), **C14AT6** (green), and **C16AT6** (blue) in 90% H_2O/10% D_2O with 10 mM phosphate buffer and 100 mM NaCl at temperatures between 5 and 40 °C .

Discussion

C12A*n* Conjugates. The selection of the C12-linker employed in the initial stages of our investigation was motivated by a report on the formation of stable dumbbell conjugates constructed using two of these linkers by Doktycz et al.[19] Hairpins possessing the C12-linker with four or more AT base pairs display well resolved melting transitions with values of $T_m \geq 25$ °C (Figure 1). A weak melting transition with T_m ca. 8 °C is observed for hairpin **C12A3**, and no melting transition is observed for **C12A2**. The CD spectra (Figure 4a) are consistent with the assignment of a B-DNA geometry for the base-pair domains. The CD spectrum for **C12A2** is also much broader than that for **C12A4** and the hairpins having longer base-paired stems (Figure 4a). The 260 nm CD shoulder characteristic of longer poly(dA)poly(dT) duplexes[24] is fully resolved only in the case of **C12A8** (Figure 4a).

Information about base pairing in the C12-linked conjugates is provided by the imino proton region of their ^{1}H 1D NMR spectra (Figure 6). In the case of **C12A8**, 6 of the 8 exchangeable imino protons are resolved in the 5 °C spectrum, indicating that two of the imino protons undergo rapid

(24) Johnson, W. C. In *Landolt-Börnstein, Group VII*; Saenger, W., Ed.; Springer-Verlag: Berlin, 1990; Vol. I, pp 1−24.

exchange at this temperature. Previous studies of base-pair opening of A-T base pairs in duplex poly(dA-dT) have shown that end effects are limited to the two terminal base pairs.[25] Thus we assume that the two base pairs at the nonlinked end of the base-pair domain undergo rapid exchange at 5 °C. In the case of **C12A6**, 3 of the 6 imino protons are resolved in the 5 °C spectrum, indicating that the imino proton of a third base pair undergoes rapid exchange. In the case of **C12A4** two of the imino protons can barely be resolved at 5 °C, indicating that opening of all of the base pairs occurs rapidly on the NMR time scale.[26] The imino protons signals for all three conjugates broaden and become weaker with increasing temperature (Figure 6), in accord with previous studies of the temperature dependence of imino proton exchange.[25]

Information about the C12 linker is provided by the high field region of the NMR spectra (0−1.5 ppm), which should contain all of the protons of the alkyl linker except for the two terminal methylenes that are attached to oxygen (Figure 7). The NMR spectra of all three hairpins have multiple resolved signals for the alkane protons in the region 0−1.0 ppm, unlike the spectrum of 1,12-dodecanediol in which the signals for the eight interior methylenes lie in a very narrow chemical shift range. The dispersion of the C12 linker signals is consistent with a structure in which the methylenes are stretched out across the top of the adjacent base pair and experience different magnetic environments from the base-pair ring currents. In the case of **C12A4**, signal dispersion for alkane methylene protons is observed in the spectra recorded at all temperatures, i.e., below and above the UV melting temperature (T_m = 25 °C). These signals do not collapse into a single chemical shift region above the melting temperature, nor do they broaden significantly, as would be expected for averaging of many different orientations of the linker with respect to the DNA bases. Two explanations for this behavior are possible: either the linker adopts a different binding mode to the dissociated bases, or the linker prevents complete opening of the adjacent base pair, retaining the same hydrophobic exclusion of the linker with the base pair as seen below T_m.

The 1D NMR spectral data for the C12-linked alkanes are consistent with the minimized structure for **C12A6** previously reported by Burin et al.[11] shown in Figure 9. A similar linker structure in which an extended alkane chain lies parallel to the adjacent base pair of a B-DNA base-pair domain was proposed by Doktycz et al. for their C12-linked dumbbell.[19] The complete assignment of the NMR spectra and the structure of a C12-linked hairpin would require 2D NMR experiments that we have not undertaken for the conjugates in this study.

C*n*A6 Conjugates. All of the C*n*A6 conjugates have similar CD spectra (Figure 4b), consistent with similar B-DNA geometries of their base-pair domains. Values of T_m for the **C*n*A6** conjugates obtained from the derivatives of their 260 nm UV (Figure 2) or CD thermal dissociation profiles (Figures 5 and S2−S4 in Supporting Information) increase with increasing linker length from n = 8 to 14 and then decrease for the longer linkers (Figure 3). Further evidence

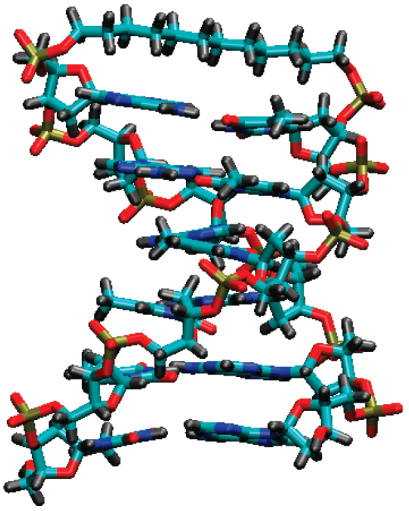

FIGURE 9. A minimized structure for **C12A6** obtained from molecular dynamics simulations (from ref 11).

for the optimum stability of the C14 linker when compared to shorter or longer alkane linkers is provided by the temperature-dependent ^{1}H NMR spectra of the exchangeable imino protons (Figure 8). Several imino protons are observed at room temperature for the C14 linker but not for either the C12 or C16 linker.

Analysis of the thermodynamics of base-pair melting is complicated by the different shapes of the melting curves of alkanes having odd versus even numbers of methylenes. Linkers containing an even number of methylenes exhibit hyperchromism at temperatures above their melting transitions as is typical of A-tract duplexes, but linkers containing an odd number of methylenes do not do so (Figure 2). We can offer no simple explanation for this difference; however, ample precedent exists for both types of melting behavior for duplex DNA.[27,28] Differences in the physical properties of odd versus even straight-chain alkanes,[29] α,ω-alkanediols,[30] and α,ω-dicarboxylic acids[31] have long been a source of fascination for organic chemists. However, there is no obvious relationship between our results and these studies.

It is interesting to compare the calculated lengths of the fully extended (all-*anti*) conformations of the alkane linkers (Table 2) with the average P−P interstrand distance in B-DNA, which is 17.7 Å.[2] This average distance is similar to that calculated for the extended C11 linker but considerably shorter than that for the C14 linker, which affords the most stable hairpin. Plausibly the longer linkers adopt multiple gauche conformations that would reduce the linker P−P distance, thus providing a better match to a normal B-DNA geometry.

Comparison with Other Non-natural Linkers. Values of T_m for the C12-linked hairpins having variable numbers of base pairs can be compared with those reported for the analogous hairpins having EG6 or Sd2 linkers (Table 1). For hairpins

(25) Leroy, J. L.; Kochoyan, M.; Huynhdinh, T.; Gueron, M. *J. Mol. Biol.* **1988**, *200*, 223–238.
(26) Moe, J. G.; Russu, I. M. *Nucleic Acids Res.* **1990**, *18*, 821–827.
(27) Owczarzy, R. *Biophys. Chem.* **2005**, *117*, 207–215.
(28) Watkins, N. E.; SantaLucia, J. *Nucleic Acids Res.* **2005**, *33*, 6258–6267.
(29) Muller, A. *Proc. Royal Soc. London A* **1929**, *124*, 317–321.
(30) (a) Thalladi, V. R.; Boese, R.; Weiss, H. C. *Angew. Chem., Int. Ed.* **2000**, *39*, 918–922. (b) Uno, K.; Ogawa, Y.; Nakamura, N. *Cryst. Growth Des.* **2008**, *8*, 592–599.
(31) Burrows, H. D. *J. Chem. Educ.* **1992**, *69*, 69–73.

with 6 AT base pairs the order of stability is EG6 < C12 < Sd2, with essentially similar values of ΔT_M = 10 °C. The most obvious explanation for this trend is the anticipated difference in extent of hydrophobic association of the linker with the adjacent base pair. The crystal structure for a Sd2-linked hairpin shows that the stilbene chromophore is π-stacked with the adjacent base pair with a plane to plane separation of 3.4 Å and P−P distance of 18.1 Å,[8] values similar to those for B-DNA. Several NMR investigations of the solution structures of EG6-linked hairpins have provided resolved structures for the base-pair domains but have failed to yield constraints for the EG6 linker.[14,32] Molecular dynamics simulations for hairpins and dumbbells having EG6 linkers have shown that all of the ethylene glycol units adopt the gauche conformation favored by unconstrained elthylene glycol oligomers,[33] resulting in a highly disordered linker geometry. In contrast, the structure obtained from molecular dynamics simulation of **C12A6** displays an extended alkyl chain approximately parallel to the adjacent base pair (Figure 9). Efforts to determine the solution structure of a C12-linked hairpin are continuing in our laboratory.

A second factor that may influence the relative stabilities of hairpins having non-natural linkers is the length of the linker. Both C12 and EG6 form slightly less stable hairpins than do their longer homologues C14 and EG7,[16] respectively. On the other hand Sd2 forms a more stable hairpin than its homologues possessing either one or two additional methylenes attached to each side of the stilbenediether.[9] A fully extended Sd2 linker would have a P−P distance of 21.9 Å similar to that calculated for the C14 linker. The incorporation of two O−C−C−O gauche conformations shortens this distance to the 18.1 Å observed in the crystal structure.[8,10] Introduction of two gauche butane conformations in C14 would result in a similar reduction in its P−P distance, plausibly accounting for the greater stability of its hairpin compared with those formed by the C12 or C16 linkers.

Concluding Remarks. We have explored the use of alkane linkers as alternatives to poly(ethylene glycol) as nonchromophoric linkers for the construction of stable short DNA hairpins. The UV, CD, and NMR spectra and molecular dynamics simulations of the alkane-linked hairpins are consistent with the formation of base-paired B-DNA hairpin structures. The stability of the alkane-linked hairpins is determined by the alkane length as well as the number of base pairs. The C14 linker forms the most stable of the alkane-linked hairpins, as evidenced both by comparison of T_m values and the temperature dependence of the imino proton region of the NMR spectrum. The length of a fully extended C14 linker is longer than the average P−P distance in DNA. Comparison of the length of this linker with that of the Sd2 linker suggests that its hairpins may incorporate two or more gauche butane conformations. The thermal stabilities of hairpins possessing the C12 linker are greater than those of hairpins possessing the extensively studied EG6 linker. However, they are less stable than hairpins possessing the Sd2 linker, which forms the most stable synthetic mini-hairpins reported to date.[9] The order of hairpin stability, Sd2 > C12 > EG6 is attributed primarily to the strength of the hydrophobic interaction with the neighboring base pair.

Unlike the linkers containing aromatic chromophores used in our studies of electron transfer, energy transfer, and exciton coupling in DNA,[34] nonchromophoric linkers permit the study of the electronic spectra and photochemical behavior of short, well-defined base-pair domains. Alkane-linked mini-hairpins possessing a single TT step have permitted us to investigate the context-dependence of T-T photodimerization,[12] a leading cause of UV damage to cellular DNA by UV light.[35] Molecular modeling of our experimental results has provided evidence in support of ground state conformational control of T-T dimerization efficiency.[13]

Experimental Section

Materials. The monoprotected, monoactivated alkane linker precursors were prepared by sequential reaction of respective α,ω-alkanediol with 4,4′-dimethoxytrityl chloride and with 2-cyanoethyl diisopropylchlorophosphoramidite as the per the literature procedure.[9,36] Hairpin sequences were synthesized by means of conventional phosphoramidite chemistry starting from 5′-phosphate CPG as solid support using a Millipore Expedite DNA synthesizer and following the procedure of Letsinger and Wu.[6] Following synthesis, the conjugates were isolated as trityl-on derivatives by reverse phase (RP) HPLC, detritylated in 80% acetic acid for 30 min, and repurified by RP-HPLC as needed (Figure S5−S7, Supporting Information). RP-HPLC analysis was carried out on a Dionex chromatograph with a Hewlett-Packard Hypersil ODS-5 column (4.6 mm × 250 mm) and a 1% gradient of acetonitrile in 0.03 M triethylammonium acetate buffer (pH 7.0) with a flow rate of 1.0 mL/min. Molecular weights were determined following desalting by means of MALDI-TOF mass spectroscopy (Tables S1 and S2, Supporting Information).

Ultraviolet Absorption and Circular Dichroism Spectra. UV spectra were obtained using a Perkin-Elmer Lambda 2 UV spectrophotometer equipped with a Peltier sample holder and a temperature programmer for automatically increasing the temperature at the rate of 0.5 °C/min. Spectra were measured for aqueous solutions of 1−1.2 μM conjugate in 10 mM phosphate buffer (pH 7.2) containing 100 mM NaCl in 1 cm path length quartz cells using single scan with a scan speed of 120 nm/min. Circular dichroism spectra were obtained using JASCO J-815 Spectropolarimeter for aqueous solutions of 2−3 μM conjugate in 10 mM phosphate buffer (pH 7.2) containing 100 mM NaCl in 1 cm path length quartz cells. Spectra were obtained from the sum of three scans over the 200−320 nm wavelength range with a scan speed of 100 nm/min, a bandwidth of 1.0 nm, and a response time of 2 s. The spectra were corrected by subtraction of a background scan obtained for the buffer solution.

NMR Spectra. Samples of hairpin sequences used for NMR experiments were lyophilized four times from aqueous NH_4-OH solution (10%) to remove residual triethylamine. The samples were dissolved in 200 μL of H_2O/D_2O (9:1), containing 100 mM NaCl and 10 mM phosphate buffer (pH 7.2), and then transferred to NMR microtubes (Shigemi Co., Tokyo,

(32) Kozerski, L.; Mazurek, A. P.; Kawecki, R.; Bocian, W.; Krajewski, P.; Bednarek, E.; Sitkowski, J.; Williamson, M. P.; Moir, A. J. G.; Hansen, P. E. *Nucleic Acids Res.* **2001**, *29*, 1132–1143.
(33) Eliel, E. L.; Wilen, S. H. *Stereochemistry of Organic Compounds*; Wiley: New York, 1994.
(34) Lewis, F. D. *Pure Appl. Chem.* **2006**, *78*, 2287–2295.
(35) (a) Beukers, R.; Berends, W. *Biochim. Biophys. Acta* **1960**, *41*, 550–551. (b) Setlow, R. B. *Science* **1966**, *153*, 379–386.
(36) Lewis, F. D.; Zhu, H.; Daublain, P.; Fiebig, T.; Raytchev, M.; Wang, Q.; Shafirovich, V. *J. Am. Chem. Soc.* **2005**, *128*, 791–800.

Japan). The final concentration of the DNA-hairpin was 0.3−0.5 mM.

NMR spectra were recorded using a Varian Inova 600 spectrometer equipped with a Cold Probe. A series of 1D spectra was recorded at temperatures of 5, 10, 20, 30, and 40 °C. All spectra were acquired in 90% H_2O/10% D_2O using the WATERGATE pulse sequence for water suppression.[37]

(37) Piotto, M.; Saudek, V.; Sklenar, V. *J. Biomol. NMR* **1992**, *2*, 661–665.

Acknowledgment. Funding for this project was provided by the National Science Foundation (NSF-CRC grant CHE-0628130).

Supporting Information Available: HPLC traces and MALDI-TOF analysis for the hairpin sequences **C12A2**−**C12A8**, **C8A6**−**C16A6**, and **C12AT6**−**C14AT6**, representative UV and temperature-dependent circular dichroism spectra of sequence **C9A6**, **C11A6**, and **C14A6**. This material is available free of charge via the Internet at http://pubs.acs.org.